

Dielectric Response of Soft Modes in Ferroelectric Thin Films

J. PETZELT, P. KUŽEL, I. RYCHETSKÝ, A. PASHKIN,
and T. OSTAPCHUK

*Institute of Physics, Academy of Sciences of the Czech Rep., Na Slovance 2,
182 21 Praha 8, Czech Republic*

(Received October 16, 2002; In final form January 30, 2003)

The concept of effective soft mode in thin films and its role in the effective dielectric response of high-permittivity thin films is introduced. Compared to bulk soft mode response, it may be strongly influenced by stresses from the substrate and dielectric inhomogeneities like interface layers, grain boundaries and porosity. The available techniques for the determination of the effective soft-mode response (far-infrared and time-domain THz spectroscopies) are discussed. The experiments on various ferroelectric (PbTiO₃, PZT, BaTiO₃, SrB₁₂Ta₂O₉), incipient ferroelectric (SrTiO₃), doped incipient ferroelectric (SrTiO₃:Ba), and relaxor ferroelectric (PLZT) films are briefly reviewed and compared with the results in bulk materials.

Keywords: Ferroelectric soft mode; thin films; effective dielectric response; far-infrared spectroscopy; time-domain THz spectroscopy; Raman spectroscopy

1. EFFECTIVE DIELECTRIC RESPONSE OF THIN FILMS

It is frequently found that ferroelectric and/or high-permittivity thin films show a smaller dielectric constant (permittivity) than bulk materials [1–3]. The reason for it may be a change of the structure due to a macroscopic residual stress owing to the substrate, but usually more serious effects are caused by dielectric inhomogeneities in the sample. In the case of standard low-frequency dielectric measurements, the most pronounced effect is as a rule the so called dead-layer effect [4]. The dead layer is a thin (a few nm) inter-phase layer between the film and the electrodes or the substrate; it shows a lower local permittivity than the film and theoretically it can be expected at any surface. A standard dielectric experiment with an applied electric field normal to the film plane is sensitive to the out-of-plane response, i.e. it measures the effective permittivity ε_{eff} , which is a result of the series

combination of film and dead layer capacitances:

$$\varepsilon_{eff}^{-1} = x_1 \varepsilon_1^{-1} + x_2 \varepsilon_2^{-1} \quad (1)$$

where $\varepsilon_1, \varepsilon_2$ are the permittivities and x_1, x_2 the relative volumes of the film and dead layer, respectively.

On the other hand, contact-less spectroscopic techniques mainly discussed in this paper probe the in-plane response, since the electric field of the radiation impinging under normal incidence is parallel to the film plane. Also microwave techniques which make use of two electrodes deposited on the top surface of the film probe essentially the in-plane response. In these cases the dead-layer effect is almost negligible since the measured capacitances are arranged in parallel so that

$$\varepsilon_{eff} = x_1 \varepsilon_1 + x_2 \varepsilon_2. \quad (2)$$

Equations (1) and (2) represent the lower and upper bounds for the effective permittivity of any two-component composite with an arbitrary shape of individual components [5].

The concept of the two-component composite can be also used for the description of the effect of various kinds of imperfections—such as grain boundaries and porosity—which are usually present in thin films and which may also significantly reduce the effective response (see below). The generalized effective medium approximation (EMA) applied to two-component composites uses the concept of percolated and non-percolated clusters of the two components [5–7]. If some clusters of one component are percolated to a macroscopic length in the direction of the external field, the depolarization field effect is negligible inside these clusters: their dielectric response does not differ from that of the bulk. For non-percolated clusters the depolarization field reduces their local response depending on their shape and neighborhood. The effective integral response of the sample then corresponds to an average value over all clusters and it always lies between the two bounds. The upper bound permittivity [Eq. (2)] is related to the situation when both components are fully percolated in the field direction, while the lower bound [Eq. (1)] describes samples with no percolated clusters of any component.

Various EMA models are used for evaluation of the effective dielectric response. The simplest one is the classical Maxwell-Garnett spherical cluster model in a percolated matrix. This model can describe for instance the effect of spherical pores in thin films and ceramics, but it leads only to a small reduction of the effective permittivity compared to the bulk one, since

nearly all the bulk (matrix) volume is percolated [7, 8]. The influence of grain boundaries in thin films can be accounted for much better in the so-called brick-wall model [9]. Assuming that the volume fraction $x_2 = 1 - x_1$ and the permittivity ε_2 of the grain boundaries are small enough, the model yields approximately:

$$\varepsilon_{eff}^{-1} = x_1 \varepsilon_1^{-1} + g x_2 \varepsilon_2^{-1} \quad (3)$$

The geometrical factor $0 < g \leq 1$ accounts for the fact that not all the boundaries are perpendicular to the probe field (e.g., for cubic grains $g = 1/3$). The essential feature of this approximate model is the vanishing percolated volume of the bulk because all the grains are mutually separated by boundaries. Hashin and Shtrikman [10] have treated analytically another geometry having this feature, so called coated-spheres geometry. It assumes that the whole sample space is filled up with various-size bulk spheres coated with spherical layers of the second component. The corresponding dielectric response reads:

$$\varepsilon_{eff} = \varepsilon_2 + \frac{3x_1 \varepsilon_2 (\varepsilon_1 - \varepsilon_2)}{3\varepsilon_2 + x_2 (\varepsilon_1 - \varepsilon_2)} \quad (4)$$

It can be shown [8] that for a small concentration of the second component ($x_2 \ll 1$) and for $\varepsilon_1 \gg \varepsilon_2$ this model becomes equivalent to that of brick walls (3) with $g = 1/3$.

The approach of EMA is valid as long as (i) the macroscopic electric field is uniform within individual clusters and (ii) the magnetic field effects may be neglected [11]. We restrict our analysis to dielectric thin films where the linear size of inhomogeneities due to the grains, their boundaries, and pores is typically of the order of 100 nm or smaller. The wavelength and the penetration depth of the far infrared (FIR) and sub-millimeter radiation largely exceed this dimension even in high-permittivity materials. Owing to these properties, the two above-mentioned conditions are fulfilled: we can thus readily use the EMA approach [i.e. Eqs. (1–4)] for the evaluation of the frequency-dependent dielectric response function within these spectral ranges and, in particular, for investigation of the soft mode behaviour.

In order to simplify the analysis, let us assume that the whole dielectric response consists of a dominant soft-mode contribution. We denote the soft mode parameters ω_{T1} (frequency) and γ_1 (damping). Let us further assume that the corresponding frequency ω_{T2} of the boundary medium is stiffened ($\omega_{T2} > \omega_{T1}$) which may be expected for the grain boundaries. One can

then show that the effective response consists of a sum of renormalized oscillators. Let us consider e.g. the coated-spheres model described by Eq. (4); the substitution for the dielectric functions ε_1 and ε_2 in (4) leads to a sum of three damped harmonic oscillators [7, 8]:

$$\varepsilon_{eff}(\omega) - \varepsilon_\infty = \frac{2x_2}{3 - x_2} \frac{g_2 \omega_{T2}^2}{\omega_{T2}^2 - \omega^2 + i\gamma_2 \omega} + \left(1 - \frac{2x_2}{3 - x_2}\right) \times \left(\frac{g_2^* \omega_{T2}^{*2}}{\omega_{T2}^{*2} - \omega^2 + i\gamma_2^* \omega} + \frac{g_1^* \omega_{T1}^{*2}}{\omega_{T1}^{*2} - \omega^2 + i\gamma_1^* \omega} \right). \quad (5)$$

The first term (oscillator) corresponds to the percolated part of the grain boundaries with unchanged frequency ω_{T2} . The second term describes the response of the grain boundaries in presence of the local (depolarization) electric field causing an increase of the eigenfrequency $\omega_{T2}^* > \omega_{T2}$. The last oscillator (which is the most important one) describes the response of the inner (non-percolated) grains: the soft-mode frequency also appears to be stiffened $\omega_{T1}^* > \omega_{T1}$. Dielectric strengths g_1, g_2 concern the bulk and grain boundaries, respectively, while g_1^*, g_2^* are renormalized dielectric strengths due to the presence of internal electric fields. Neglecting the dampings, for small concentrations x_2 and for $\varepsilon_{1,\infty} = \varepsilon_{2,\infty} = \varepsilon_\infty$, with longitudinal eigenfrequencies $\omega_{L1}^2 = \omega_{T1}^2(1 + g_1 \varepsilon_\infty^{-1})$ and $\omega_{L2}^2 = \omega_{T2}^2(1 + g_2 \varepsilon_\infty^{-1})$ one obtains:

$$\omega_{T2}^2 < \omega_{T2}^{*2} = \omega_{L2}^2 - \frac{x_2 (\omega_{L2}^2 - \omega_{T2}^2)(\omega_{L2}^2 - \omega_{L1}^2)}{3 (\omega_{L2}^2 - \omega_{T1}^2)} < \omega_{L2}^2$$

$$\omega_{T1}^2 < \omega_{T1}^{*2} = \omega_{T1}^2 + \frac{x_2 (\omega_{L1}^2 - \omega_{T1}^2)(\omega_{T2}^2 - \omega_{T1}^2)}{3 (\omega_{L2}^2 - \omega_{T1}^2)} < \omega_{L1}^2. \quad (6)$$

The renormalized dielectric strengths fulfill relations $0 \leq g_1 - g_1^* \propto x_2, g_2^* \propto x_2$ so that $g_2^* \ll g_1^* \leq g_1$ and therefore the last oscillator in (5) represents the dominant term. In addition, the proportionality constant between $g_1 - g_1^*$ and x_2 is found to be rather high in high-permittivity materials. A considerable decrease of effective permittivity is then expected even for small values of x_2 . In the cases when a part of the first component is percolated (e.g. Maxwell-Garnett model), the FIR spectrum may contain up to four damped harmonic oscillators [7]. The additional mode is characterized by the original soft mode frequency ω_{T1} , its strength is proportional to the volume of the percolated component.

Concluding this part, it has been shown that the FIR spectroscopy of thin high-permittivity films may provide quite useful information about the static dielectric response and physical reasons of its possible reduction.

2. EXPERIMENTAL TECHNIQUES FOR SOFT MODE STUDIES IN THIN FILMS

Two different techniques are available for studying the soft-mode response in thin films: Raman scattering and FIR spectroscopy. Both can provide information about the soft-mode eigenfrequency and damping, but only the latter technique is also able to measure the dielectric strength, i.e. it gives access to both real and imaginary components of the complex dielectric function.

As to the Raman scattering, back-scattering geometry in the micro-Raman configuration is successfully used: the incoming laser beam is focused down to $\sim 2 \mu\text{m}$ in order to minimize the signal from the substrate. Moreover, scanning across the film may provide information about the homogeneity of the film. In the case of Raman scattering, the effective-medium response discussed in Sec. 1 cannot be applied since the depolarization field effects may influence only the UV absorption processes, which result in small variation of the optical refractive index contributing to the elastic light scattering only. Therefore one can expect some differences between the measured Raman and FIR soft-mode response in granular and/or porous films and ceramics.

So far, the FIR spectroscopy of thin films has been used mostly in normal transmission geometry. For this purpose FIR translucent substrates without electrodes and conducting buffer layers are needed. The suitable substrates are e.g. sapphire, MgO, SiO₂ (quartz or silica), LaAlO₃ and pure insulating Si; the optimum thickness ranges between 0.3 and 0.5 mm [12].

In the standard Fourier transform (FT) FIR interferometry, two methods of evaluation are used [12, 13]. A simplified one makes use of averages over the interference oscillations due to the multiple passage through the sample (substrate) or filters them out mathematically from the interferogram. The used approximation consists in dividing such a smoothed spectrum by the smoothed spectrum of the bare substrate: the resulting ratio (transmission function) is then fitted to an expression for a sum of classical damped oscillators in a single-slab. The rigorous evaluation first requires fitting the bare-substrate spectrum to obtain its dielectric function. Only after that the sample spectrum can be fitted using a general formula for a two-slab system including all interferences. Our estimates show that the simplified approach

is justified in the cases of small and medium values of the film permittivity and absorption. For higher values, typical of proper ferroelectric soft modes ($\epsilon \geq 100$), the simplified method underestimates the oscillator strength (by several tens of per cent); on the other hand, the frequencies and dampings of the fitted modes are almost not affected.

The transmission study may be combined with normal reflectance measurements to avoid the model fitting and allow a direct calculation of the complex dielectric function (or complex refractive index). Trial tests show comparable results to those obtained by fitting; however, no published FIR results using this procedure are available so far. If an opaque metallic layer is on the bottom of the film, the reflectance spectra only can be measured and fitted with appropriate formulas [13]. A reliable calculation of the dielectric function of the film requires knowing the properties of the underlying metal with a good precision: it is not always possible to describe the properties of the metal by those of a simple Drude conductor.

An important accuracy improvement of the FT FIR technique at its long-wavelength edge is achieved by more sensitive modern submillimetre techniques which use coherent radiation. The earlier one is based on monochromatic tunable backward-wave-oscillator (BWO) sources, the more recent one—time-domain THz spectroscopy (TDTS)—utilizes ultrashort broadband THz pulses generated usually by photoconductive switches excited with femtosecond lasers. Both techniques enable measuring the amplitude as well as the phase shift of the transmitted wave; therefore the complex dielectric response can be calculated without any model assumption [14]. Very recently, reflectance measurements have also become available using both the techniques. In our lab we extensively use the TDTS technique, therefore we shall briefly discuss its specific features and derive basic formulas for the thin films.

The experimental setup we use for TDTS is schematically shown in Fig. 1. It requires a laser system delivering femtosecond pulses (time duration typically 100 fs). The output of the laser is divided into two beams: the first beam pumps the emitter, which produces ultrashort transients of freely propagating THz radiation [15, 16]. The second beam, which passes through a variable delay line, is used for the gated photoconductive [17] or electro-optic [16] detection. The delay scans allow measuring the time profile of the electric field of the THz pulse. The spectroscopic method applied to thin films consists in two consecutive measurements: (i) measurement of a signal waveform $E_s(t)$ with the sample (thin film on a substrate) in the path of the THz beam and (ii) measurement of a reference waveform $E_r(t)$ with an empty sample holder or with a bare substrate. The spectra of the two signals

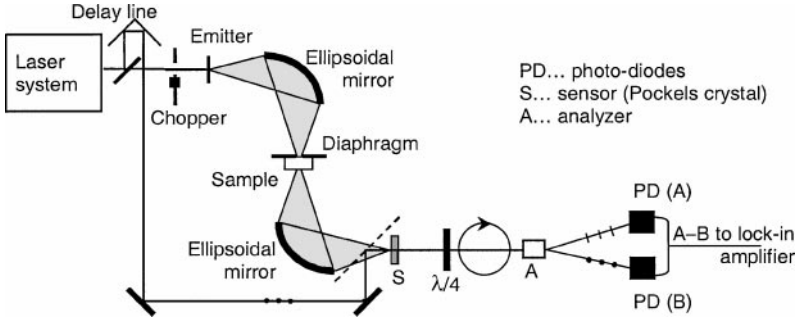


Figure 1. Scheme of our experimental setup for the time-domain THz transmission spectroscopy.

are obtained through the Fourier transformation and their ratio defines the complex transmission function:

$$t(\omega) = E_s(\omega)/E_r(\omega). \quad (7)$$

For thick substrates (THz optical thickness larger than about 0.7 mm) the internal Fabry-Pérot reflections in the substrate are resolved in time and form separate pulses in the measured signal. One then usually proceeds to the temporal windowing of the signal, i.e. the calculations are made using one particular reflection cut off from the temporal waveform. If we consider the directly transmitted pulse only (i.e. all the Fabry-Pérot reflections inside the substrate are cut off) and if the reference measurement is performed with the bare substrate, the transmission function reads:

$$t(\omega) = \frac{2N_f(N_s + 1) \exp[i\omega(N_f - 1)d_f/c] \exp[i\omega(N_s - 1)(d_s - d'_s)/c]}{(1 + N_f)(N_f + N_s) + (1 - N_f)(N_f - N_s) \exp[2i\omega N_f d_f/c]}, \quad (8)$$

where c is the speed of the light, N_f and d_f are the complex refractive index and the thickness of the thin film, respectively, and N_s and d_s are the refractive index and the thickness of the underlying substrate. The thickness of the bare substrate used for the reference measurement was denoted as d'_s . Usually $\omega N_f d_f/c \ll 1$; within this approximation Eq. (8) can be further simplified and the refractive index of the thin film can be expressed analytically:

$$N_f^2 = \frac{ic(1 + N_s)}{\omega d_f} \left[\frac{1}{t(\omega)} \frac{\exp[i\omega(N_s - 1)(d_s - d'_s)/c]}{(1 + i\omega d_f/c)} - 1 \right] - N_s. \quad (9)$$

Similar equations can be derived for the experiment where the reference measurement is performed with an empty sample holder. In particular, within the thin film approximation one obtains:

$$N_f^2 = \frac{ic(1 + N_s)}{\omega d_f} \left[\frac{1}{t(\omega)} \frac{4N_s \exp[i\omega(N_s - 1)d_s/c]}{(1 + N_s)^2(1 + i\omega d_f/c)} - 1 \right] - N_s. \quad (10)$$

In both these cases the precision of the output data depends very critically on the determination of the film and substrate thicknesses.

- (i) The film thickness d_f appears practically as a multiplication factor in the denominator of Eqs. (8) and (9): d_f directly scales the value of the dielectric constant. An error in d_f thus can distort the soft mode strength; on the other hand, neither the value of the soft mode frequency nor that of its damping are influenced by this error.
- (ii) The phase change that the THz pulse acquires due to propagation through the substrate is much larger than that due to the propagation through the thin film. The uncertainty in the phase of $t(\omega)$ owing to the substrate should be kept as small as possible:

$$N_s \Delta d_s + (d_s - d'_s) \Delta N_s < N_f d_f, \quad (11)$$

where Δd_s is the error in the substrate thickness and ΔN_s is the uncertainty in its refractive index determination. It then follows that the dielectric properties of thin films can be more easily determined near resonances, where N_f is large, than in the regions of transparency; the precision also decreases when the film thickness decreases. A special care should be devoted to the substrate preparation (parallelism of input and output faces) and to the determination of its thickness. The error in d_s can be efficiently minimized e.g. if the thin film is deposited only onto a part of the substrate plate: the uncoated part then can serve for the reference measurement.

If the phase uncertainty of $t(\omega)$ is too large, the qualitative shape of $N_f(\omega)$ obtained from Eqs. (9) or (10) will remain correct, however, the mean value of N_f and the oscillator strengths will be wrong. In such a case it can be useful to disregard the phase and to fit the amplitude of $t(\omega)$ to a model together with the FT FIR transmission data.

As an example, dielectric permittivity and losses of thin SrTiO₃ (ST) and Ba_{0.1}Sr_{0.9}TiO₃ (BST 10/90) films on sapphire substrate calculated according to simplified approach (Eq. (9)) are compared with a model dielectric response obtained by fitting of FT FIR transmission measurements in Fig. 2.

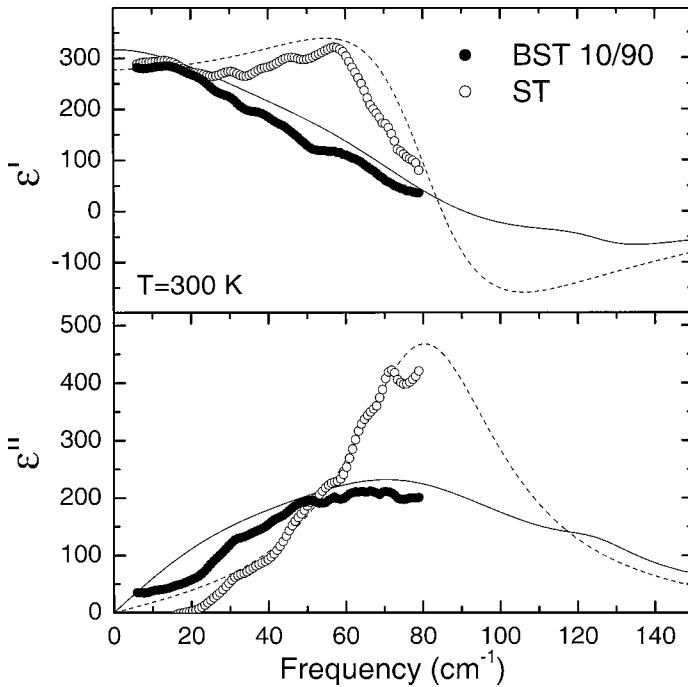


Figure 2. Permittivity and losses of BST 10/90 and ST thin films obtained with the help of TDTS (circles) and calculated from the fit of FT FIR transmittance spectra (lines).

Further improvement of the thin-film measurements can be achieved by TDTS using the reflection geometry, recently developed in our laboratory [18]. The THz pulse reflected from the sample mostly probes the dielectric properties of the thin film. The calculated permittivity of the film is then less sensitive to the uncertainty in the refractive index of the substrate and insensitive to the uncertainty in its thickness.

RESULTS

Our earlier data were already reviewed in other recent papers [12, 19, 20], therefore we discuss the results here briefly, mainly in context of some interesting new aspects. Until now, the FIR thin-film soft-mode studies in our lab have concerned the following compounds:

1. PZT system (PZT 53/47 and 75/25) including pure PbTiO_3 (PT) [21], PbZrO_3 (PZ) [22] and three La doped PZT (PLZT 9.5/65/35 [23], 8/65/35 [24] and 2/95/5 [24]); features observed in PT will be reviewed in this paper.
2. BST system including pure BaTiO_3 (BT) [12, 20, 25], ST [26–30] BST 35/65, 65/35 [27] and 10/90 [20, 25, 31]; phenomena observed in ST will be discussed here.
3. $\text{SrBi}_2\text{Ta}_2\text{O}_9$ (SBT) [32].

In all the cases studied a strong low-frequency (below $\sim 100 \text{ cm}^{-1}$) polar mode was detected; it is revealed by a pronounced transmission minimum at a frequency corresponding to the maximum of losses and it dominates the dielectric function. It should be stressed that such feature is found even in the case of overdamped modes for which the corresponding Raman spectra yield only central peaks. As a matter of fact, the accuracy of evaluation of the soft mode parameters decreases with increasing damping, nevertheless, the FIR transmission spectroscopy provides here more accurate results than the Raman scattering. This is particularly true near ferroelectric phase transitions where the Raman intensity of soft modes mostly approaches zero since they are usually (i.e. in the case of inversion symmetry) Raman-forbidden in the paraelectric phase.

Lead Titanate (PT) Thin Films

The data on PT [21] were the first published FIR data on ferroelectric thin films. The E-symmetry component of the split soft-mode doublet was investigated from room temperature up to 920 K, and a good agreement was obtained with the corresponding Raman frequencies detected in a single crystal by Burns and Scott [33]. However, the effective dielectric function calculated using the simple EMA model with spherical grains (i.e. assuming macroscopically isotropic polycrystal with bulk mode parameters) based on the complete single-crystal Raman data [33] in the range of $0\text{--}250 \text{ cm}^{-1}$ did not show a good agreement with the fitted FIR dielectric function. A new assignment by Foster *et al.* [34] showed that the bulk-crystal soft mode at room temperature is split more than it was assumed earlier [33] into the E-component ($E \perp c$) at 88 cm^{-1} and A_1 -component ($E \parallel c$) at 149 cm^{-1} . A proper treatment of these two modes by the above EMA theory with the relative volumes of $2/3$ and $1/3$, respectively, leads to an effective stiffening of the A_1 mode in a polycrystal [35]. The fit based on FT FIR and BWO transmission measurements in polycrystalline thin films [21] yielded 86 and

161 cm^{-1} , respectively and a good agreement with EMA theory was obtained. Therefore we cannot agree with a more recent paper by Fu et al. [36] who ignored the result of Fedorov [35] and used the earlier assignment for the fitting of their Raman data obtained on a polycrystalline PT thin film.

Most of the Raman data on PT films indicate that the E-component of the soft mode has the resonance frequency reduced by $\sim 10\%$ compared to single crystals [36, 37 and references therein]. This is attributed to hydrostatic compressive micro-stresses due to the clamping of anisotropic tetragonal grains on cooling from the cubic phase above T_c ($\sim 763 \text{ K}$ in single crystals). In favour of this interpretation Yuzyuk et al. [37] showed that the difference between the Raman soft-mode frequencies in film and crystal substantially decrease on heating to T_c in correlation with the temperature dependent tetragonal deformation. It was also pointed out that the Raman strength of the soft mode remains non-zero in quite a broad interval above T_c . This is caused by clamping of the film by the substrate, which is the reason of slight macroscopic tetragonal distortion even in the paraelectric phase. Also, T_c was found to be shifted down (by $\sim 15\text{--}20 \text{ K}$) due to the compressive micro-stresses discussed above [36, 37].

Strontium Titanate (ST) Thin Films

The most interesting results have been recently achieved on ST films [30]. Our laboratory was the first to notice that the soft mode in thin films does not soften on cooling so much as in single crystals [26]; this effect also leads to a reduction of the low-temperature static permittivity in ST films. In fact, the soft-mode frequency levels off completely below the structural transition near 105 K and the corresponding maximum of losses broadens. This observation has been confirmed on several differently processed ST films [27–29] and also by FIR ellipsometry [38] and electric-field-induced Raman scattering [39], however, it remained unexplained until recently.

Our most recent experiment [30] has been carried out on stoichiometric films grown on a (0001) sapphire substrate: the first sample (STO1) was a quasi-epitaxial MOCVD 290 nm thick film and the other two samples were polycrystalline sol-gel films differing only by their thicknesses (STO2 – 360 nm and STO3 – 690 nm). A higher stress in STO1 film (tensile in-plane strain of 0.17%) compared to STO2 (0.10%) and to STO3 (0.04%) was caused by a larger thermal dilatation of ST compared to the substrate (not by the lattice mismatch which is large and has the opposite sign). All

the films were granular (grain size ~ 100 nm), but in the case of STO1 just two types of single-crystalline (111)-oriented grains mutually rotated by 60° appeared whereas the columnar grains observed in STO2 and STO3 were nearly randomly oriented.

The soft-mode behaviour in STO1 revealed that the film undergoes a macroscopic ferroelectric transition (with P_s in the film plane) combined with the antiferrodistortive one near 125 K. Such a change of the phase diagram due to the tensile stress can be expected from the theory [40]. Saturation of the static permittivity (slightly above the value of 1000) below this transition is caused by the ferroelectric soft-mode hardening combined with the IR activation of the structural soft-mode doublet through the coupling with the former mode (see Fig. 3).

In contrast, the polycrystalline films (STO2 and STO3) did not show any macroscopic phase transition (but local polar regions are evidenced by micro-Raman spectra up to room temperature, probably due to the effect of polar grain boundaries [41]). The soft mode was stiffened compared to single crystals in the whole 10–300 K temperature range; this stiffening was

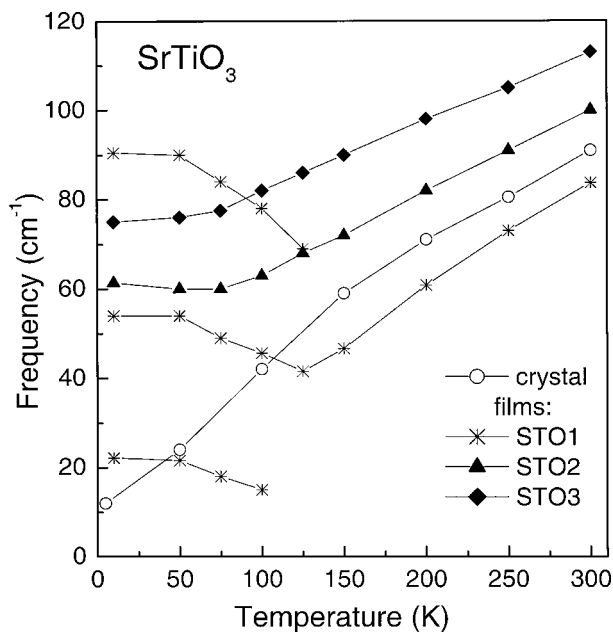


Figure 3. Soft mode frequencies in STO1, 2, 3 films versus temperature compared with the single-crystal ones.

pronounced appreciably more in the thicker STO3 film than in the STO2 one (Fig. 3). Scanning electron microscopy showed quite a lot of porosity along the grain boundaries on the fracture of both these films and optical and atomic-force microscopy revealed nanometer cracks along some of the grain boundaries in the STO3 film. Application of the brick-wall model to describe the influence of cracks showed that 0.2 and 0.4% of air-crack-type porosity (independent of temperature) is enough to account for the observed soft-mode behaviour in STO2 and STO3, respectively (see Fig. 4). The latter amount is in agreement with the observed cracks assuming their thickness is about 10 nm. It means that in thicker sol-gel films the tensile stresses are relaxed by nano-cracking along some of the grain boundaries and this increases the effective soft-mode frequency and substantially reduces the in-plane dielectric response.

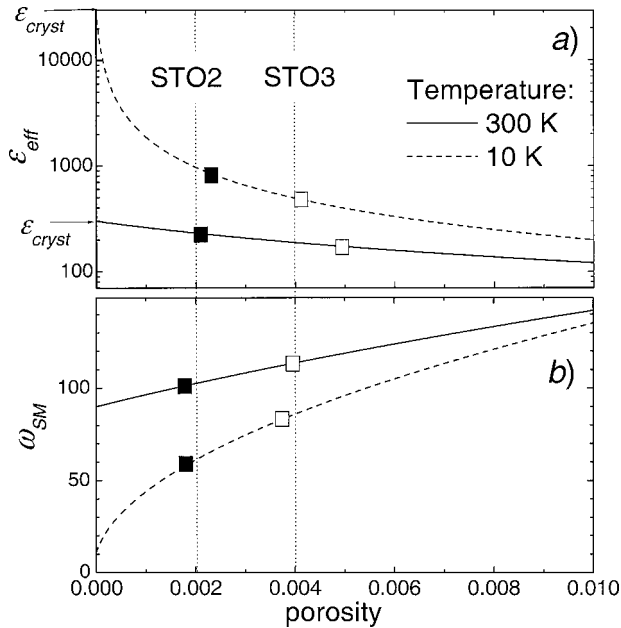


Figure 4. Effective permittivity (a) and the corresponding soft-mode frequency (b) versus volume fraction of the crack-type porosity, calculated using the brick-wall model (Eq. (3)) with $g = 1/2$ (columnar geometry) for the two extreme temperatures. Our measured data correspond to 0.2 and 0.4% porosity for STO2 and STO3, respectively, independently of temperature.

Summarizing, the main causes of the reduction of the dielectric response in ST thin films are interfacial layers, the residual stresses (which may also induce ferroelectric phase transition—at least locally), the grain boundaries (always present in films with thickness of hundreds nm), and porosity, particularly the nano-cracks. The impact of these effects increases dramatically with increasing permittivity, therefore, in the case of ST, they are dominant at low temperatures.

Strontium Bismuth Tantalate (SBT) Thin Films

Our last reported and most recent results [32] were obtained on the SBT films, the first non-perovskite ferroelectric film (of Aurivillius bilayered pseudo-perovskite structure) studied. SBT is a high-temperature proper ferroelectric with $T_c \sim 600$ K and a recently revealed improper ferroelastic phase from ~ 600 to ~ 780 K [42]. The bulk underdamped soft mode softens only incompletely from 27 cm^{-1} at 20 K to $\sim 21\text{ cm}^{-1}$ at 550 K [42]. In Fig. 5 we show our fit to room-temperature FT FIR transmission data on a $5.1\text{ }\mu\text{m}$ thick film on sapphire substrate compared with the independently measured data using TDTS [32]. The soft mode frequency is close to its bulk value, but as expected, its damping is higher and strength by $\sim 30\%$ lower compared with bulk parameters.

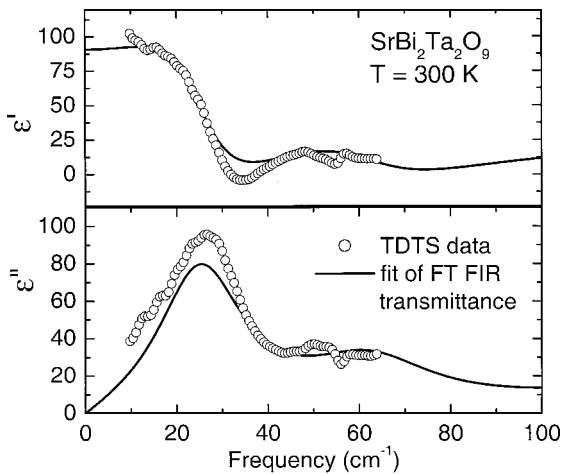


Figure 5. Real and imaginary parts of dielectric function of SBT film (thickness $5.1\text{ }\mu\text{m}$) in the soft-mode range at room temperature.

CONCLUSION

Concluding, we now understand much better what are the principal reasons for reducing the dielectric response and shifting the soft-mode frequency in thin films. Besides the well-accepted dead-layer effects and possible non-stoichiometry, we have shown the dramatic consequences of the effect of grain boundaries, and particularly pores and nano-cracks along the boundaries. Finally, it was shown that residual strains may induce ferroelectricity in incipient ferroelectrics. The quantitative soft-mode spectroscopy proved to be a very useful and sensitive method for determining the film quality and analyzing the physical reasons for its diminution compared to bulk materials.

The work was supported by the Czech grant agencies GACR (projects No. 202/01/0612, 202/02/0238, and 202/00/1187), GAAS (project No. A1010213 and AVOZ1-010-914) and Czech Ministry of Education (project COST OC 525.20/00).

REFERENCES

- [1] H.-M. Christen, J. Mannhart, and E. J. Williams, and Ch. Gerber, "Dielectric properties of sputtered SrTiO₃ films," *Phys. Rev. B* **49**, 12095–12104 (1994).
- [2] H.-C. Li, W. Si, A. D. West, and X. X. Xi, "Thickness dependence of dielectric loss in SrTiO₃ thin films," *Appl. Phys. Lett.* **73**, 464–466 (1998).
- [3] D. Fuchs, C. W. Schneider, R. Schneider, and H. Rietchel, "High dielectric constant and tunability of epitaxial SrTiO₃ thin film capacitors," *J. Appl. Phys.* **85**, 7362–7369 (1999).
- [4] C. Zhou and D. M. Newns, "Intrinsic dead layer effect and the performance of ferroelectric thin film capacitors," *J. Appl. Phys.* **82**, 3081–3088 (1997).
- [5] D. J. Bergman and D. Stroud, Physical Properties of Macroscopically Inhomogeneous Media. In: H. Ehrenreich, D. Turnbull, eds. *Solid State Physics*, Vol. 46. Academic Press, Boston, 1992: 147–269.
- [6] O. Hudák, I. Rychetský, and J. Petzelt, "Dielectric response of microcomposite ferroelectrics," *Ferroelectrics* **208/209**, 429–447 (1998).
- [7] I. Rychetský, O. Hudák, and J. Petzelt, "Dielectric properties of microcomposite ferroelectrics," *Phase Transitions* **67**, 725–739 (1999).
- [8] I. Rychetský, J. Petzelt, and T. Ostapchuk, "Grain-boundary and crack effects on the dielectric response of high-permittivity films and ceramics," *Appl. Phys. Lett.* **81**, 4224–4226 (2002).
- [9] M. H. Frey, Z. Xu, P. Han, and D. A. Payne, "The role of interfaces on an apparent grain size effect on the dielectric properties for ferroelectric barium titanate ceramics," *Ferroelectrics* **206/207**, 337–353 (1998).
- [10] Z. Hashin and S. Shtrikman, "A variational approach to the theory of the effective magnetic permeability of multiphase materials," *J. Appl. Phys.* **33**, 3125–3131 (1962).
- [11] I. Rychetský and J. Petzelt, "Dielectric properties of ferroelectric powders and micro-composites," *Ferroelectrics* **236**, 223–234 (2000).

- [12] J. Petzelt and T. Ostapchuk, "Far-infrared ferroelectric soft mode spectroscopy on thin films," *Ferroelectrics* **249**, 81–88 (2000).
- [13] V. Železný, I. Fedorov, and J. Petzelt, "FIR spectroscopic studies of ferroelectric films," *Czech. J. Phys.* **48**, 537–545 (1998).
- [14] G. Grüner (ed.), *Millimeter and Submillimeter Wave Spectroscopy of Solids*, Chapters 2 and 3 (Springer-Verlag Berlin Heidelberg, 1998).
- [15] B. B. Hu, J. T. Darrow, X.-C. Zhang, D. H. Auston, and P. R. Smith, "Optically steerable photoconducting antennas," *Appl. Phys. Lett.* **56**, 886–888 (1990).
- [16] A. Nahata, A. S. Weling, and T. F. Heinz, "A wideband coherent terahertz spectroscopy system using optical rectification and electro-optic sampling," *Appl. Phys. Lett.* **69**, 2321–2323 (1996).
- [17] Ch. Fattering and D. Grischkowsky, "Point source terahertz optics," *Appl. Phys. Lett.* **53**, 1480–1482 (1988).
- [18] A. Pashkin, H. Němec, M. Kempa, F. Kadlec, and P. Kužel, to be published.
- [19] J. Petzelt, T. Ostapchuk, and S. Kamba, Ferroelectric soft-mode spectroscopy in disordered bulk and thin-film perovskites. In: G. Borstel, et al., eds. *Defects and Surface-Induced Effects in Advanced Perovskites*. NATO Science Ser. 3. High technology 77. Dordrecht: Kluwer Acad. Publ. 233–248 (2000).
- [20] J. Petzelt and T. Ostapchuk, "Soft-mode spectroscopy in SrTiO₃, BaTiO₃ and BST films and ceramics," *Ferroelectrics* **267**, 93–100 (2002).
- [21] I. Fedorov, J. Petzelt, V. Železný, G. A. Komandin, A. A. Volkov, K. Brooks, Y. Huang, and N. Setter, "Far-infrared dielectric response of PbTiO₃ and PbZr_{1-x}Ti_xO₃ thin ferroelectric films," *J. Phys. Condens. Matter* **7**, 4313–4323 (1995).
- [22] T. Ostapchuk, J. Petzelt, V. Železný, S. Kamba, B. Malič, M. Kosec, L. Čakare, K. Roleder, and J. Dec, "Infrared spectroscopy of lead zirconate crystal, ceramics and films," *Ferroelectrics* **239**, 109–115 (2000).
- [23] I. Fedorov, J. Petzelt, V. Železný, A. A. Volkov, M. Kosec, and U. Delalut, "The submillimetre dielectric response of a PLZT 9.5/65/35 relaxor thin film," *J. Phys. Condens. Matter* **9**, 5205–5216 (1997).
- [24] T. Ostapchuk, V. Železný, J. Petzelt, B. Malič, and M. Kosec, "Infrared spectroscopy of thin PLZT films," *SPIE Proc. Characterization of Dielectric Materials* **37DP**, 156–161 (1999).
- [25] J. Petzelt, T. Ostapchuk, A. Pashkin, and I. Rychetský, "FIR and near-millimetre dielectric response of SrTiO₃, BaTiO₃ and BST films and ceramics," *J. Eur. Cer. Soc.* in press.
- [26] I. Fedorov, V. Železný, J. Petzelt, V. Trepakov, M. Jelínek, V. Trtík, M. Čerňanský, and V. Studnička, "Far-infrared spectroscopy of a SrTiO₃ thin film," *Ferroelectrics* **208–209**, 413–127 (1998).
- [27] V. Železný, J. Petzelt, K. Kämmer, "Infrared spectroscopy of laser deposited Ba_xSr_{1-x}TiO₃ films," *J. Kor. Phys. Soc.* **32**, S1615–S1617 (1998).
- [28] J. Petzelt, T. Ostapchuk, S. Kamba, I. Rychetský, M. Savinov, A. Volkov, B. Gorshunov, A. Pronin, S. Hoffmann, R. Waser, and J. Lindner, "High-frequency dielectric response of SrTiO₃ crystals, ceramics and thin films," *Ferroelectrics* **239**, 117–124 (2000).
- [29] J. Petzelt, T. Ostapchuk, I. Gregora, S. Hoffmann, J. Lindner, D. Rafaja, S. Kamba, J. Pokorný, V. Bovtun, V. Porokhonsky, M. Savinov, P. Vaněk, I. Rychetský, V. Peřina, and R. Waser, "Far-infrared and Raman spectroscopy of ferroelectric soft mode in SrTiO₃ thin films and ceramics," *Integrated Ferroelectrics* **32**, 11–20 (2001).
- [30] T. Ostapchuk, J. Petzelt, V. Železný, A. Pashkin, J. Pokorný, I. Drbohlav, R. Kužel, D. Rafaja, B. P. Gorshunov, M. Dressel, Ch. Ohly, S. Hoffmann-Eifert, and R. Waser, "Origin

- of the soft-mode stiffening and reduced dielectric response in SrTiO₃ thin films," *Phys. Rev. B* **66**, 235406–1/12 (2002).
- [31] A. Pashkin, P. Kužel, J. Petzelt, B. Gorshunov, and M. Dressel, "Time-resolved and backward-wave oscillator submillimetre spectroscopy of some ferroelectric ceramics and thin films," *Ferroelectrics* **272**, 219–224 (2002).
- [32] S. Kamba, et al. to be published.
- [33] G. Burns and B. A. Scott, "Lattice modes in ferroelectric perovskites: PbTiO₃," *Phys. Rev. B* **7**, 3088–3101 (1973).
- [34] C. M. Foster, Z. Li, M. Grinditch, S.-K. Chan, and D. J. Lam, "Anharmonicity of the lowest frequency A₁(TO) phonon in PbTiO₃," *Phys. Rev. B* **48**, 10160–10167 (1993).
- [35] I. Fedorov, "Application of the effective medium theory to ferroelectric thin films," *Sol. State Commun.* **103**, 347–350 (1997).
- [36] D. S. Fu, H. Iwazaki, H. Suzuki, and K. Ishikawa, "Phonon mode behaviours of PbTiO₃ thin films deposited on Pt/Si substrates," *J. Phys. Condens. Matter.* **12**, 399–414 (2000).
- [37] Y. I. Yuzuyk, R. Farhi, V. L. Lorman, L. M. Rabkin, L. A. Sapoznikov, E. V. Sviridov, and I. N. Zakharchenko, "A comparative Raman study of ferroelectric PbTiO₃ single crystal and thin film prepared on MgO substrate," *J. Appl. Phys.* **84**, 452–457 (1998).
- [38] A. A. Sirenko, C. Bernrhard, A. Golnik, A. M. Clark, J. Hao, W. Si, and X. X. Xi, "Soft-mode hardening in SrTiO₃ thin films," *Nature* **404**, 373–376 (2000).
- [39] I. A. Akimov, A. A. Sirenko, A. M. Clark, J. H. Hao, and X. X. Xi, "Electric-field induced soft-mode hardening in SrTiO₃ films," *Phys. Rev. Lett.* **84**, 4625–4628 (2000).
- [40] N. A. Pertsev, A. K. Tagantsev, and N. Setter, "Phase transitions and strain-induced ferroelectricity in SrTiO₃ epitaxial thin films," *Phys. Rev. B* **61**, R825–R829 (2000). N. A. Pertsev, A. K. Tagantsev, and N. Setter, "Erratum: Phase transitions and strain-induced ferroelectricity in SrTiO₃ epitaxial thin films," *Phys. Rev. B* **65**, 219901 (2002).
- [41] J. Petzelt, T. Ostapchuk, I. Gregora, I. Rychetský, S. Hoffmann-Eifert, A. V. Pronin, Y. Yuzuyk, B. P. Gorshunov, S. Kamba, V. Bovtun, J. Pokorný, M. Savinov, V. Porokhonsky, D. Rafaja, P. Vaněk, A. Almeida, M. R. Chaves, A. A. Volkov, M. Dressel, and R. Waser, "Dielectric, infrared and Raman response of undoped SrTiO₃ ceramics: Evidence of polar grain boundaries," *Phys. Rev. B* **64**, 184111-1/10 (2001).
- [42] S. Kamba, J. Pokorný, V. Porokhonsky, J. Petzelt, M. P. Moret, A. Garg, Z. H. Barber, and R. Zallen, "Ferroelastic phase in SrBi₂Ta₂O₉ and study of the ferroelectric phase-transition dynamics," *Appl. Phys. Lett.* **81**, 1056–1058 (2002).

Copyright of Ferroelectrics is the property of Taylor & Francis Ltd and its content may not be copied or emailed to multiple sites or posted to a listserv without the copyright holder's express written permission. However, users may print, download, or email articles for individual use.